Multiphase control of a nonlinear lattice

M. Khasin and L. Friedland
Racah Institute of Physics, Hebrew University of Jerusalem, Jerusalem 91904, Israel
(Received 25 July 2003; published 31 December 2003)

Large amplitude, multiphase excitations of the periodic Toda lattice (n-gap solutions) are created and controlled by small forcing. The approach uses passage through an ensemble of resonances and subsequent multiphase self-locking of the system with adiabatic wavelike perturbations. The synchronization of each phase in the excited lattice proceeds from the weakly nonlinear stage, where the problem can be reduced to that for a number of independent, driven, one-degree-of-freedom oscillatory systems. Due to this separability, the phase locking at this stage is robust, provided the amplitude of the corresponding forcing component exceeds a threshold, which scales as 3/4 power of the corresponding frequency chirp rate. The adiabatic synchronization continues into a fully nonlinear stage, as the driven lattice self-adjusts its state to remain in a persisting and stable multifrequency resonance with the driving perturbation. Thus, a complete control of the n-gap state becomes possible by slow variation of external parameters.

DOI: 10.1103/PhysRevE.68.066214 PACS number(s): 05.45.Xt

I. INTRODUCTION

Integrable and near-integrable nonlinear systems comprise a foundation for modeling and understanding a large variety of nonlinear phenomena [1]. Therefore, finding realizable methods of excitation and control of different coherent states in these systems is one of the main goals of nonlinear science. In many cases, one knows that a certain nontrivial solution in a nonlinear system exists, but its realization requires satisfaction of very complicated initial/boundary conditions, making these states practically unaccessible. For example, some one-dimensional systems [2] possess multiphase solutions described by nontrivial nonlinear functions of many variables (phases), all of form $kx-\omega t$, with different wave vectors k and frequencies ω in each phase. The question is how to excite and control one of such solutions.

Recently, in a number of applications in extended systems [3–7], a new approach to realization of some of nontrivial coherent states was suggested. The idea was based on starting from a simple, easily realizable equilibrium and adding a special driving perturbation, such that the desired nontrivial state of the system was reached in the process of evolution. In particular, in Ref. [7], multiphase solutions of the Korteweg–de Vries (KdV) equation were excited from zero by a perturbation in the form of a superposition of waves with slowly varying frequencies, passing through multiple resonances in the system. It was found that under certain conditions, the perturbed KdV system multiphase locked (synchronized) with the driving perturbation, yielding a large excursion in the solutions space, as the driving frequencies varied in time. Due to this synchronization, a complete control of a multiphase state of the KdV system was achieved by slow variation of external parameters. In the present work we apply similar ideas to excitation and control of multiple degrees of freedom of a periodic Toda lattice.

The Toda lattice [8] is one of the most studied dynamical systems. It is a chain of unit masses, each interacting with its two neighbors via exponential interaction potential. Weakly nonlinear approximations to the lattice played an important role in the resolution of the Fermi-Pasta-Ulam (FPU) paradox [9,10]. The continuum limit of the lattice allowed a convenient approach to nonlinear partial differential equations, contributing to the development of the modern nonlinear science of systems of many degrees of freedom. The integrability of the Toda lattice was proven by Henon [11] and Flaschka [12], and its initial value problem comprised one of the famous applications of the inverse scattering transform method [13,14]. The Toda lattice and its various approximations continue to attract scientific attention with applications in mathematical physics [15], statistical physics [16], condensed matter [17], and soliton physics [18,19], to name just few recent examples. In the present work, we focus on the N-periodic Toda lattice and pose a question of how to strongly excite a desired number $n(n<N)$ of degrees of freedom (each characterized by its action-angle variables) in the system by starting with the lattice at rest and applying synchronizing, adiabatically varying perturbations. We seek a continuing multiphase locking in the system, accompanied by a large (but reversible) deformation of the driven solution, yielding a desired nontrivial state in the process of evolution.

The scope of our presentation will be as follows. We shall illustrate our approach by numerical simulations in Sec. II. We shall consider $N=5$ periodic lattice example and show that a desired number of degrees of freedom in the system can be excited, provided the amplitudes of the corresponding components in the synchronizing perturbation of a particular type exceed certain thresholds. We shall analyze this threshold phenomenon in Sec. III, showing that the thresholds are characteristic signatures of resonant trapping by passage through multiple resonances in the weakly nonlinear stage of evolution of our system. We shall also show that the weakly nonlinear limit of the driven periodic Toda lattice can be represented by $N-1$ *decoupled* driven anharmonic oscillators. As a consequence, each degree of freedom can be excited *independently*. This will allow us to use the existing results for one-degree-of-freedom synchronized systems in calculating the multiphase synchronization thresholds for the Toda lattice. Section IV will present our theory of a fully nonlinear synchronized evolution of the driven lattice. Also, in Sec. IV, the theoretical scaling of frequencies of small

modulations of synchronized states versus driving amplitudes will be tested numerically. Finally, Sec. V will present our conclusions.

II. SYNCHRONIZED EXCITATIONS VIA NUMERICAL SIMULATIONS

The N-particle periodic Toda lattice is described by the Hamiltonian

$$H_0=\sum_{n=1}^{N}\left[\frac{1}{2}p_n^2+\exp(q_n-q_{n+1})\right], \tag{1}$$

where q_n is the displacement of the nth mass from equilibrium and $q_{N+1}=q_1$. The lattice is a completely integrable dynamical system [11,12] possessing famous g-gap solutions, which can be written in terms of the Riemann ϑ function [20]:

$$p_n=p_0+\frac{d}{dt}\ln\frac{\vartheta(n\mathbf{c}-\mathbf{c}'t+\mathbf{\Delta})}{\vartheta((n+1)\mathbf{c}-\mathbf{c}'t+\mathbf{\Delta})}$$

$$q_n=q_0+p_0t+\ln\frac{\vartheta(n\mathbf{c}-\mathbf{c}'t+\mathbf{\Delta})}{\vartheta((n+1)\mathbf{c}-\mathbf{c}'t+\mathbf{\Delta})}, \tag{2}$$

where p_0, q_0, $\mathbf{c}=(c_1,c_2,\ldots,c_g)$, $\mathbf{c}'=(c_1',c_2',\ldots,c_g')$, and $\mathbf{\Delta}=(\Delta_1,\Delta_2,\ldots,\Delta_g)$ are constants defined by initial conditions. These solutions are nontrivial 2π-periodic functions of g phases of form $2\pi nk/N-\omega_k t$, with the set of g integers $k\in\{1,2,\ldots,N-1\}$ and corresponding frequencies ω_k. We shall denote this set of integers by I_g and use dimensionless time t in the following. The initial value problem for the periodic Toda lattice is mathematically complex and realization of a multigap state with, say, a given set of frequencies requires very special initial conditions. Consequently, these solutions are almost entirely dealt with on an advanced mathematical level [13,14,20]. Nevertheless, we shall show that adding a weak forcing and starting with zero initial conditions, one can conveniently excite and control multigap solutions. Our driving perturbation is a superposition of g small amplitude ''traveling waves,'' such that the force on the nth particle is

$$f_n(t)=\frac{1}{\sqrt{N}}\sum_{k\in I_g}\varepsilon_k\cos\left[\frac{2\pi nk}{N}-\Phi_k(t)\right]. \tag{3}$$

Here $\Phi_k(t)=\int^t\Omega_k(t)dt$ are defined by slowly varying frequencies $\Omega_k(t)$, all passing, at, say $t=0$, through resonances with the unperturbed lattice, i.e., $\Omega_k(0)=\omega_k^0=2\sin(\pi k/N)$ [8], thus coupling the kth phase in the drive with the kth phase of q_n. The number of phases (or open gaps in the main spectrum, see below) in the excited solution will correspond to the number of terms in the drive, while the frequencies and amplitudes of the emerging solution will be controlled by local values of the chirped driving frequencies.

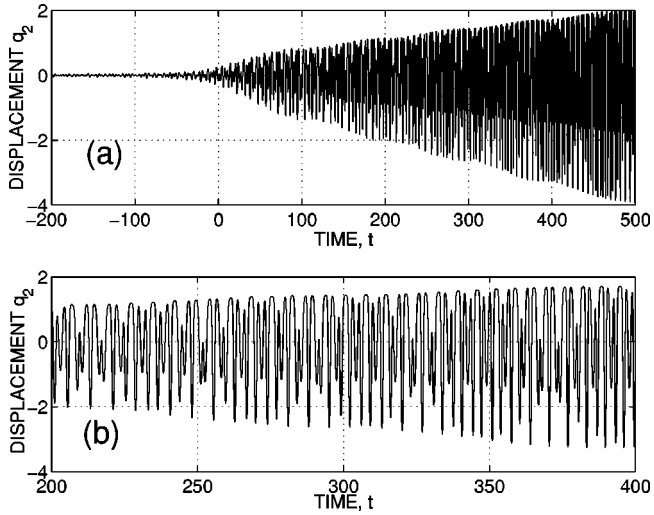

FIG. 1. The emergence of a two-gap solution in the periodic five-particle Toda lattice. (a): Displacement q_2 of the second atom in the lattice vs time t. (b): Displacement q_2 in shorter time window, $200<t<400$.

We proceed by presenting results of numerical simulations illustrating our ideas. Figure 1 shows emergence of a two-phase solution for the driven, $N=5$ periodic Toda lattice described by the Hamiltonian

$$H=H_0+\sum_{n=1}^{N}q_nf_n. \tag{4}$$

We used zero initial conditions and two driving components in Eq. (3), having amplitudes $\varepsilon_{1,2}=0.045$, 0.074, phases with $k=1,2$, and linearly chirped frequencies $\Omega_{1,2}(t)=\omega_{1,2}^0+\alpha_{1,2}t$, with chirp rates $\alpha_{1,2}=0.0020$, 0.0028. The figure shows evolution of the displacement q_2 of the second atom in the lattice. One observes that the excited motion is rather complex. Nevertheless, we see the growth of the amplitude of oscillations well into the nonlinear stage, despite the smallness of the driving amplitudes $\varepsilon_{1,2}$. For diagnostics of these numerical results, we used spectral tools from the theory of the unperturbed, periodic Toda lattice [8]. We shall briefly describe these tools below for completeness.

In addition to representation (2), the g-gap solutions governed by Hamiltonian (1) can be written as [8]

$$p_n=\sum_{i=1}^{2g+2}\lambda_i-2\sum_{i=1}^{g}\mu_i(t), \tag{5}$$

where all λ and μ are defined in terms of three linear eigenvalue problems of the associated discrete Hill's equation

$$(L\cdot\psi)_n\equiv a_{n-1}\psi_{n-1}+b_n\psi_n+a_n\psi_{n+1}=\lambda\psi_n, \tag{6}$$

where $a_n=\frac{1}{2}\exp[-(q_{n+1}-q_n)/2]$ and $b_n=\frac{1}{2}p_n$. The set $\{\lambda_i\}$ (the so-called *main spectrum*) in Eq. (5) is the combination of two sets of eigenvalues $\{\lambda^+\}$ and $\{\lambda^-\}$ in Eq. (6), corresponding to the periodic ($\psi_{n+N}=\psi_n$) and antiperiodic ($\psi_{n+N}=-\psi_n$) boundary conditions, respectively. In contrast, $\{\mu_i\}$ (the *auxiliary spectrum*) in Eq. (5) is the set of eigenvalues corresponding to zero boundary conditions, $\psi_N=\psi_1=0$. It is known [8] that the auxiliary spectrum μ de-

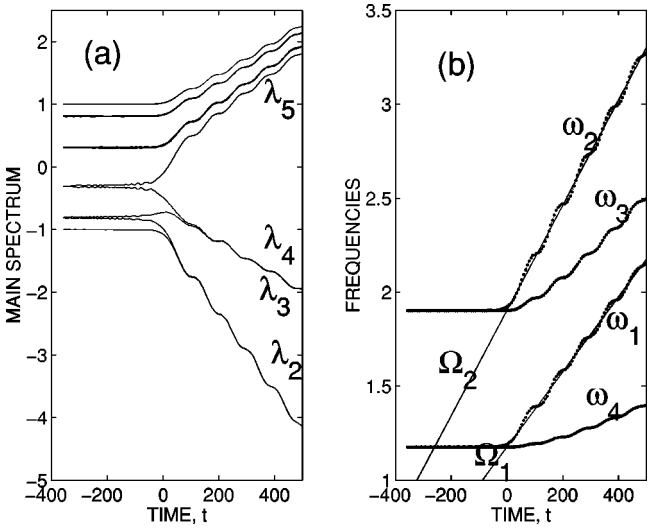

FIG. 2. The spectral analysis of the driven five-particle periodic Toda lattice. (a) The opening of two main spectrum gaps $[\lambda_2,\lambda_3]$ and $[\lambda_4,\lambda_5]$ by passage through resonance and synchronization. (b): The frequencies ω_n of the excited wave (dots) and chirped driving frequencies $\Omega_{1,2}$ (straight lines).

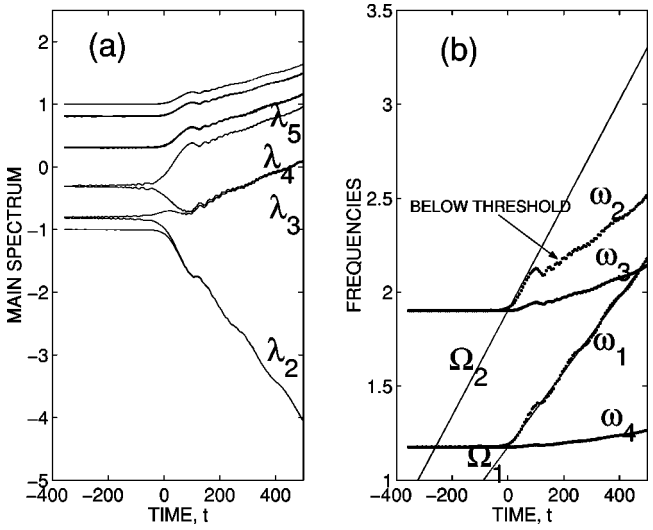

FIG. 3. The threshold phenomenon. The parameters and initial conditions are the same as in Fig. 2, but the driving amplitude ε_2 is below the threshold. (a): The widening of the gap $[\lambda_4,\lambda_5]$ is stopped shortly beyond the linear resonance. (b): The frequencies ω_n of the excited wave (dots) and chirped driving frequencies $\Omega_{1,2}$ (straight lines). The resonance between ω_2 and the chirped frequency Ω_2 is discontinued.

pends on time, while the main spectrum $\lambda \equiv \{\lambda^+,\lambda^-\}$ is time independent and, therefore, can be found from initial conditions. The structure of the spectra of the *g*-gap solution is as follows. If all $2N$ values λ of the main spectrum are ordered by their values, i.e., $\lambda_1 \leqslant \lambda_2 \leqslant \cdots \leqslant \lambda_{2N}$, then the strict inequality $\lambda_{2k} < \lambda_{2k+1}$ holds for g values of $k \in I_g$ only. The intervals $[\lambda_{2k},\lambda_{2k+1}]$ are called *gaps* in the main spectrum. We associate the auxiliary spectrum components with these gaps as follows. When $\lambda_{2k}=\lambda_{2k+1}$ (the gap is closed), then there exists μ_k in the auxiliary spectrum, satisfying $\mu_k = \lambda_{2k} = \lambda_{2k+1}$ and, thus, this component remains constant in time. In contrast, when $[\lambda_{2k},\lambda_{2k+1}]$ gap is open, there exists a corresponding μ_k, which oscillates between λ_{2k} and λ_{2k+1}, i.e., $\lambda_{2k} \leqslant \mu_k(t) \leqslant \lambda_{2k+1}$.

At this stage, we use the spectral machinery described above in analyzing properties of our *driven* solution. Since the driving perturbation remains small throughout our calculation, we view our numerical solution, at each *t*, as a local approximation to some solution of the unperturbed problem. Within this interpretation, we substitute the numerical solution into Eq. (6), view *t* as a parameter, calculate the main spectrum $\lambda(t)$ of the *approximating* lattice, and show the evolution of λ in Fig. 2(a). In contrast to Fig. 1, the spectral data in Fig. 2(a) reveal simple structure and evolution. We see the opening of two gaps at linear resonances ($t=0$), followed by the adiabatic increase of the width of each gap. Given the main spectrum λ, the spectral theory also allows us to calculate the associated frequencies ω_n (see definitions in Ref. [21]) of the multigap solution. The dotted lines in Fig. 2(b) show the evolution of ω_n, while the chirped driving frequencies are represented by straight lines. One observes that in average, starting $t \approx 0$, both frequencies $\omega_{1,2}$ follow the corresponding, linearly increasing driving frequencies, indicating a continuing phase locking (resonance) in the driven system. In contrast, one finds that the remaining two frequencies $\omega_{3,4}$ increase quadratically in time, just beyond $t=0$. We shall show in Sec. III that this characteristic evolution of those frequencies of the lattice, which are not represented in the drive, indicates separability of the weakly nonlinear driven lattice problem into a set of *independent*, one-degree-of-freedom problems. In addition to the slow averaged evolution, we also observe oscillatory modulations of both λ and ω_n in Fig. 2. These slow modulations are additional characteristic signatures of the persistent phase locking in the system and have frequencies scaling with the driving amplitudes as $O(\varepsilon^{1/2})$ (see Sec. IV).

The *passage through* linear resonances is an important stage for entering synchronized nonlinear evolution. Indeed, our simulations show that the phase locking is established during this early stage and sustained at later times, provided each driving amplitude exceeds a threshold. The thresholds ε_n^c scale with the chirp rates as $\alpha_n^{3/4}$ (see the following section). We illustrate this phenomenon in Fig. 3, showing the results obtained by using the same $\alpha_{1,2}$ and ε_1 as in Fig. 2, but $\varepsilon_2 = 0.059$, i.e., below the threshold value $\varepsilon_2^c = 0.062$. One observes the departure of ω_2 from resonance beyond $t=0$ in this case, i.e., the loss of phase locking with the second driving component. The first phase remains locked with the corresponding drive, but the *independent* control of both degrees of freedom becomes impossible.

In summarizing the spectral analysis of our numerical results, we conclude that in the phase locked state our driven solution approximates, at each time *t*, some excitation of the unperturbed lattice, satisfying the resonance conditions $\Omega_n(t) \approx \omega_n(t)$, $n=1,2$, provided the driving amplitudes exceed certain thresholds. Since ω_n are functions of λ, the approximating solution self-adjusts its main spectrum to stay in resonance with the drive, as the driving frequencies vary

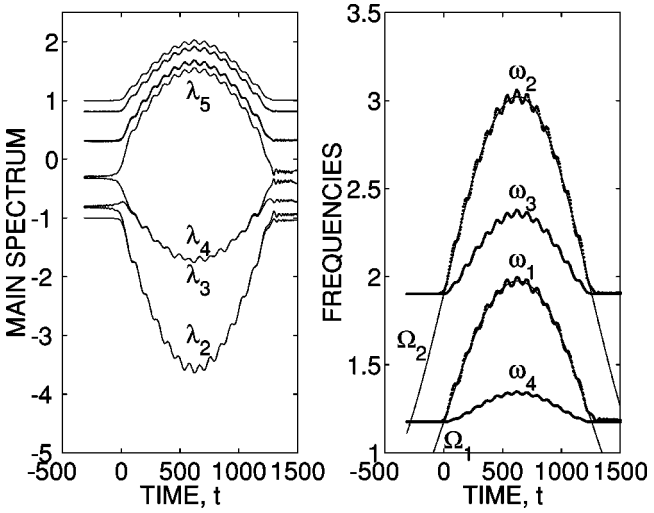

FIG. 4. The excitation and deexcitation of a two-gap solution for sinusoidal dependence of driving frequencies $\Omega_{1,2}$. (a): The opening and near closure of two gaps in the main spectrum. (b): The frequencies ω_n of the excited wave (dots) and chirped driving frequencies $\Omega_{1,2}$ (thin lines). The resonance $\omega_{1,2}\approx\Omega_{1,2}$ is preserved when the driving frequencies $\Omega_{1,2}$ are above the corresponding linear frequencies, $\omega_{1,2}^0$.

in time. In other words, the system modifies the open gaps' boundaries, affecting the amplitudes of μ oscillations as well. Finally, we have found in simulations that using the linear chirp of the driving frequencies in Figs. 1–3 was just a convenient choice. In principle, the time dependence of the driving frequencies $\Omega_n(t)\equiv d\Phi_n(t)/dt$ could be arbitrary, but slow, allowing a complete control of the excited solution by chirping the frequencies of the weak forcing appropriately. We demonstrate such a control in Fig. 4, showing the excitation and deexcitation of a two-gap solution of $N=5$ periodic Toda lattice, by first increasing and then decreasing the driving frequencies as $\Omega_n(t)=\omega_n^0+d_n\sin(\alpha_n t/d_n)$. We used the same initial conditions, $\varepsilon_{1,2}=0.045$, 0.074, and $\alpha_{1,2}=0.0020$, 0.0028 as in Fig. 2, while parameters $d_{1,2}=0.8$,1.12 were such that the driving frequencies passed the corresponding linear frequencies at the same time ($t=0$ and $t=1250$ in the Fig. 4). We observe the opening and the near closure of two gaps $[\lambda_2,\lambda_3]$ and $[\lambda_4,\lambda_5]$ in the main spectrum in Fig. 4(a), as the system goes in and out of double resonance, when the driving frequencies pass the linear resonances in opposite directions at $t=0$ and $t=1250$. Figure 4(b) illustrates satisfaction of the continuing resonance condition $\omega_n(t)\approx\Omega_n(t)$ in the system during the time when $\Omega_n(t)>\omega_n^0$. The system almost returns to its initial, zero energy state beyond $t=1250$.

III. THE THRESHOLD PHENOMENON

The theory of thresholds for synchronization by passage through resonance was developed in a number of applications in driven dynamical and extended systems [22–26]. These studies showed that the thresholds are characteristic of weakly nonlinear stages of evolution of the driven systems. Furthermore, all previously studied cases allowed reduction of the problem to passage through resonance in some effective, weakly nonlinear, one-degree-of freedom dynamical system, where the scaling of the threshold with parameters could be found. We shall see here that a similar reduction exists in the periodic Toda lattice case, i.e., the weakly nonlinear limit of the driven lattice allows separation into an ensemble of *independent* one-degree-of-freedom, driven unharmonic oscillator problems.

The weakly nonlinear limit of the driven Toda lattice can be conveniently approached by making canonical transformation to the action-angle variables of the unperturbed problem. The existence of the action-angle variables $(\mathbf{I},\boldsymbol{\Theta})$ for the unperturbed periodic Toda lattice is the direct result of integrability. The formalism was developed by Flaschka and McLaughlin [21] and we shall use some results of this theory later. At this point, the fact of existence of the action-angle variables is sufficient. Generally, the unperturbed N-mass periodic Toda lattice has N actions. One action is associated with the conserved total momentum P. Since our driving perturbation (3) still conserves P, we shall assume, without loss of generality, that $P=0$ and work with $N-1$ remaining action variables corresponding to nonzero frequencies. In the linear limit, the unperturbed Hamiltonian $H_0(\mathbf{I})$ of the lattice is linear in action variables, i.e., $H_0=\Sigma_{i=1}^{N-1}I_i\omega_i^0$. The next order approximation is

$$H_0=\sum_{i=1}^{N-1} I_i\omega_i^0+\frac{1}{2}\sum_{i,j=1}^{N-1} a_{ij}I_iI_j, \tag{7}$$

yielding first-order nonlinear corrections to the linear frequencies:

$$\omega_k=\frac{\partial H_0}{\partial I_k}=\omega_k^0+\sum_{i=1}^{N-1} a_{ik}I_i. \tag{8}$$

Our goal is to find coefficients a_{ik} in these expansions. Rather than using direct transformation to action-angle variables, we shall accomplish this goal by using harmonic decomposition approach [27] applied to the evolution equations for the original displacements:

$$\frac{d^2q_n}{dt^2}=\exp[-(q_n-q_{n-1})]-\exp[-(q_{n+1}-q_n)]. \tag{9}$$

The salient feature of this approach is that it only requires knowledge of the linear limit of the canonical transformation from $(\mathbf{p},\mathbf{q})$ to $(\mathbf{I},\boldsymbol{\Theta})$ for finding nonlinear frequencies (8) to first order in action variables. In turn, the knowledge of the frequencies yields the weakly nonlinear Hamiltonian (7), sufficient for studying the threshold phenomenon.

Now, we describe our calculation of a_{ik} in more detail. We show in Appendix A that q_n in the linear limit are related to the action-angle variables [21] by

$$q_n=\sum_{l=1}^{N-1}\sqrt{\frac{2I_l}{N\omega_l^0}}\cos\left(\frac{2\pi ln}{N}-\Theta_l\right), \tag{10}$$

where $\Theta_l = \omega_l^0 t + \Theta_l^0$, while $\omega_l^0 = 2\sin(\pi l/N)$ and Θ_l^0 are the linear frequencies of the lattice and initial phases. This expression allows us to proceed with harmonic decomposition [27]. We seek a solution of Eq. (9) as a series of successive approximations

$$q_n = q_n^{(1)} + q_n^{(2)} + q_n^{(3)} + \cdots, \tag{11}$$

where the terms are ordered in increasing powers of nonlinearity. In studying the coupling between a given (i,k) pair of degrees of freedom, we assume the first-order approximation of form

$$q_n^{(1)} = \sqrt{\frac{2I_i}{N\omega_i^0}}\cos\Delta_n^i + \sqrt{\frac{2I_k}{N\omega_k^0}}\cos\Delta_n^k, \tag{12}$$

where $\Delta_n^m = 2\pi mn/N - \omega_m t - \Theta_m^0$, $m = i,k$, with frequencies ω_m including higher-order corrections:

$$\omega_m = \omega_m^{(0)} + \omega_m^{(1)} + \omega_m^{(2)} + \cdots. \tag{13}$$

We substitute ansatz (11)–(13) into Eq. (9), expand the right-hand side (RHS) of this equation to third order in powers of $q_{n+1} - q_n$, and solve the resulting equation order by order. This procedure yields successive corrections to the linear solution and frequencies. The method is straightforward, but involves tedious algebra. Thus, we used MATHEMATICA [28] to show that all nondiagonal coefficients a_{ik}, $i \neq k$ vanish, while the derivation of the diagonal coefficient a_{kk} is presented in Appendix C. The final result is simple:

$$a_{ik} = \frac{1}{2N}\delta_{ik}. \tag{14}$$

Then, the weakly nonlinear Hamiltonian (7) of the lattice assumes the following form:

$$H = \sum_{i=1}^{N-1}\left(I_i\omega_i^0 + \frac{I_i^2}{4N}\right), \tag{15}$$

i.e., the unperturbed problem is separable to second order in action variables. This also means (see the developments below) that the problem of thresholds for synchronization by passage through resonances in the driven periodic Toda case reduces to that for $N-1$ *independent* anharmonic oscillators.

It is interesting to observe that the separability of the weakly nonlinear Hamiltonian of the Toda lattice in the action variables is characteristic of the fourth-order expansion of the original Hamiltonian in powers of $q_{n+1} - q_n$. The separability is destroyed if one stops at the third order in the expansion. For example, in the pioneering studies [29–32], the choice of the lattice Hamiltonian was

$$H = \frac{1}{2}\sum_{i=1}^{N} p_i^2 + \frac{1}{2}\sum_{i=0}^{N}[q_{i+1} - q_i]^2 + \frac{\alpha}{3}\sum_{i=0}^{N}[q_{i+1} - q_i]^3, \tag{16}$$

with $\alpha = 1/2$ corresponding to the Toda potential expanded to third order in displacements. In this case, we find

$$a_{ik} = \delta_{ik}\frac{4 - (\omega_k^0)^2}{8N} + (1 - \delta_{ik})\frac{\omega_i^0\omega_k^0}{4N}. \tag{17}$$

Thus, the addition of the quartic term $(q_{i+1} - q_i)^4$ in the expansion of Hamiltonian (1) contributes the same order correction in the frequencies as the cubic term. However, this addition also simplifies the weakly nonlinear problem significantly by yielding separability. By similar arguments, the separability is destroyed if one neglects the cubic terms, but leaves the quartic terms in the expansion of the Toda potential (the FPU-β model).

Next, we consider our resonantly driven problem governed by Hamiltonian

$$H = H_0(\mathbf{I}) + \sum_{n=1}^{N} q_n(\mathbf{I},\boldsymbol{\Theta}) f_n, \tag{18}$$

where force f_n on the nth mass is defined in Eq. (3). The lowest-order expression (10) for q_n can be used in the perturbed part of this Hamiltonian, because of the assumed smallness of f_n. We recall that our driving perturbation is a superposition of g traveling waves having phases $2\pi nk/N - \Phi_k(t)$, where $k \in \{1,2,\ldots,N-1\}$ is in a set of g integers (denoted by I_g), while the driving frequencies $\Omega_k(t) = d\Phi_k/dt = \omega_k^0 + \alpha_k t$ all pass (at $t=0$) through the resonance with the corresponding g linear frequencies of the unperturbed lattice. This form of the driving perturbation allows excitation of the g-gap solution, characterized by g nonzero action variables (see Appendix A for the correspondence between the number of nonzero actions and the number of open gaps in the main spectrum). As the last preparatory step in studying passage through resonances in our system, we use the standard isolated resonance approximation [33], leaving g resonant terms only in the interaction part of the Hamiltonian, i.e., consider dynamics governed by

$$H_r = \sum_{i=1}^{N-1}\left(I_i\omega_i^0 + \frac{I_i^2}{4N}\right) + \sum_{k\in I_g}\varepsilon_k\sqrt{\frac{I_k}{2\omega_k^0}}\cos\Psi_k, \tag{19}$$

where $\Psi_k \equiv \Theta_k - \Phi_k(t)$ is the phase mismatch.

The isolated resonance Hamiltonian (19) yields the following evolution equations:

$$\frac{dI_k}{dt} = \varepsilon_k\sqrt{\frac{I_k}{2\omega_k^0}}\sin\Psi_k,$$

$$\frac{d\Psi_k}{dt} = \frac{I_k}{2N} - \alpha_k t + \frac{\varepsilon_k}{2\sqrt{2\omega_k^0 I_k}}\cos\Psi_k, \tag{20}$$

where $k \in I_g$. The rest of the actions remain zero (our initial condition on all actions) throughout the excitation process, and the corresponding gaps in the spectral theory remain closed. We observe that the evolution of each pair (I_k, Ψ_k) in Eqs. (20) is *independent* of other such pairs, and, therefore, we deal with passage through resonance in g decoupled one-degree-of-freedom systems. This allows us to write thresh-

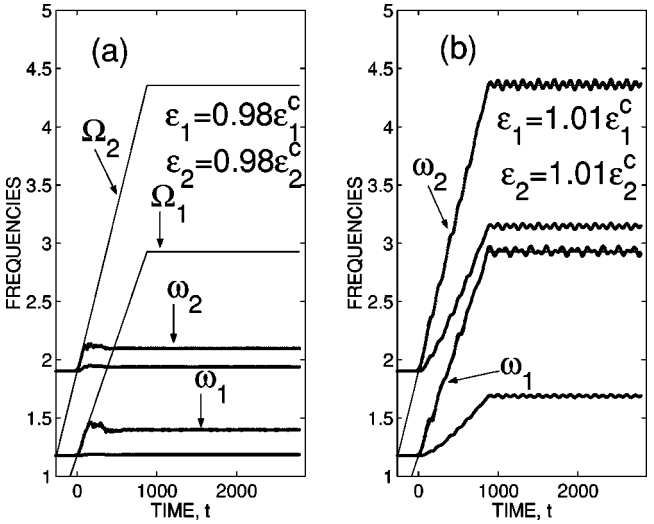

FIG. 5. The threshold phenomenon for the two-gap solution in $N=5$ Toda lattice. The driving frequencies $\Omega_{1,2}$ (thin lines) and the frequencies of the lattice $\omega_{1,2,3,4}$ (thick lines) are shown for the cases when both driving amplitudes $\varepsilon_{1,2}$ are either (a) below or (b) above the thresholds.

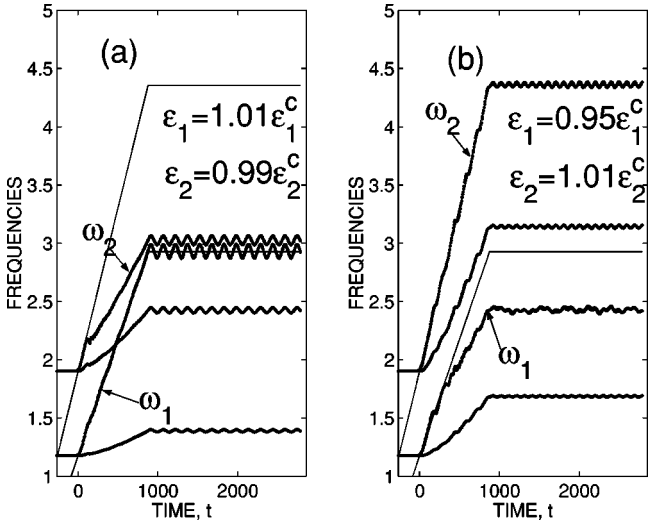

FIG. 6. Decoupling of thresholds. The driving frequencies $\Omega_{1,2}$ (thin lines) and the frequencies of the lattice $\omega_{1,2,3,4}$ (thick lines) are shown for the same parameters as in Fig. 4, but for either (a) only amplitude ε_2 slightly above the threshold or (b) only amplitude ε_1 slightly above the threshold.

olds ε_k^c for synchronization for each degree of freedom separately by using the existing theory [22]:

$$\varepsilon_k^c = 1.644\alpha_k^{3/4}\sqrt{N\omega_k^0}. \tag{21}$$

Thus, we predict multiphase locking in the system, established in the weakly nonlinear stage of evolution for each phase present in the drive independently, provided the corresponding driving amplitude exceeds threshold value (21). If the phase locking persists in the fully nonlinear stage of evolution (see the following section), as the driving frequencies continue to change, we achieve our goal of controlling the excited *g*-gap state of the periodic Toda lattice by varying external parameters. We illustrate these predictions in Figs. 5 and 6. The figures show the results of the spectral analysis of the numerical two-gap solution for the driven $N=5$ periodic lattice with four different choices of the driving amplitudes $\varepsilon_{1,2}$. In all cases, we used two linearly chirped driving frequencies $\Omega_{1,2}=\omega_{1,2}^0+\alpha_{1,2}t$ for $t<880$, while beyond $t=880$ the driving frequencies were kept constant. The corresponding chirp rates $\alpha_{1,2}=0.002$, 0.0028 were the same in all cases. Figure 5(a) shows the evolution of the frequencies for $\varepsilon_{1,2}=0.98\varepsilon_{1,2}^c$. We see that the phase locking is lost in the early stage of evolution. Figure 5(b), in contrast, depicts the evolution of the frequencies when both driving amplitudes are just above the thresholds $\varepsilon_{1,2}=1.01\varepsilon_{1,2}^c$. We observe that a stable phase locking ($\omega_{1,2}\simeq\Omega_{1,2}$) continues into the strongly nonlinear stage. In Figs. 6(a) and 6(b) we further illustrate the decoupling of the thresholds for each degree of freedom. The figure shows two cases with similar parameters as in Fig. 5, but when only one of the driving amplitudes is above its threshold, i.e., for $\varepsilon_1=0.95\varepsilon_1^c$, $\varepsilon_2=1.01\varepsilon_2^c$ and $\varepsilon_1=1.01\varepsilon_1^c$, $\varepsilon_2=0.99\varepsilon_2^c$ respectively. In both cases only one phase in the excited solution is phase locked to the corresponding driving component.

IV. SYNCHRONIZED EVOLUTION

At this stage, we proceed to fully nonlinear evolution of synchronized *g*-gap solutions. In studying this problem, we apply the spectral approach mentioned in Sec. II. We associate with our driven lattice, at each time *t*, another, *unperturbed* lattice (the approximating lattice in the following), such that its main spectrum is defined by substituting the driven solution into the eigenvalue equation (6), which we rewrite here for convenience as follows:

$$(L\cdot\psi)_n \equiv a_{n-1}\psi_{n-1}+b_n\psi_n+a_n\psi_{n+1}=\lambda\psi_n. \tag{22}$$

Here

$$a_n=\tfrac{1}{2}\exp[-(q_{n+1}-q_n)/2],\quad b_n=\tfrac{1}{2}p_n \tag{23}$$

are given by our *driven* solutions $q_n(t),p_n(t)$ and time t serves as a parameter in the spectral problem. Recall that the main spectrum in Eq. (22) is a set of eigenvalues $\lambda\equiv\{\lambda^+,\lambda^-\}$, with λ^+ corresponding to periodic $\psi_{n+N}=\psi_n$ and λ^- to antiperiodic $\psi_{n+N}=-\psi_n$ boundary conditions, respectively. Next, we seek the description of the dependence of λ of the approximating lattice on parameter *t*.

Let ψ^k be the orthonormal eigenvector corresponding to eigenvalue λ_k of Eq. (22). Then

$$\lambda_k=\psi^{k\dagger}\cdot L\cdot\psi^k. \tag{24}$$

By differentiating this expression and using the Hermiticity of L and orthonormality of ψ^k, we obtain

$$d\lambda_k/dt=\psi^{k\dagger}\cdot(dL/dt)\cdot\psi^k. \tag{25}$$

The spectral theory of the unperturbed Toda lattice (see Refs. [12,14], and [8]) uses another matrix B (the second operator in the Lax pair) defined by

$$(B\cdot\psi)_n \equiv a_{n-1}\psi_{n-1} - a_n\psi_{n+1}. \tag{26}$$

One can show that in the unperturbed problem

$$dL/dt = [B,L], \tag{27}$$

where $[B,L]\equiv B\cdot L - L\cdot B$. A similar result for dL/dt also holds in our case, but one must take into account the forcing, which yields additional diagonal terms in Eq. (27). Indeed, by using the definitions (22) and (23), one finds

$$\frac{dL_{nn}}{dt} = \frac{1}{2}\frac{dp_n}{dt}. \tag{28}$$

Therefore, the presence of external force f_n on the nth mass modifies Eq. (27) to

$$\frac{dL}{dt} = [B,L] + \frac{1}{2}F, \tag{29}$$

where $F_{nm} = f_n\delta_{nm}$. By substituting Eq. (29) into Eq. (25) we arrive at the desired system of evolution equations:

$$\frac{d\lambda_k}{dt} = \psi^{k\dagger}\cdot[B,L]\cdot\psi^k + \frac{1}{2}\psi^{k\dagger}\cdot F\cdot\psi^k. \tag{30}$$

Here, by definition of ψ^k, the first term vanishes and, therefore (compare to similar developments for the KdV equation [34])

$$\frac{d\lambda_k}{dt} = \frac{1}{2}\sum_n f_n|\psi_n^k|^2, \quad k=1,2,\ldots,2N. \tag{31}$$

Note that the main spectrum components λ_k for the approximating lattice are not independent and set λ^+ determines set λ^- and vice versa [8]. Therefore, the evolution equations for either λ^+ or λ^- are sufficient, reducing the number of independent equations (31) to N. Also, we have shown that g driving components in Eq. (3) open g gaps only. This adds $(N-1)-g$ relations:

$$\lambda_{2k_j} = \lambda_{2k_j+1}, \tag{32}$$

where index k_j corresponds to the closed gaps ($j=g+1,g+2,\ldots,N-1$). Finally, one additional relation between the main spectrum components [8],

$$P = 2\sum_{k=1}^{2N}\lambda_k^+ = 0, \tag{33}$$

reflects conservation of the total momentum P in the driven system, and we are left with g *independent* equations (31) for the main spectrum. The RHS in Eqs. (31) is of $O(\varepsilon)$, ε being a small parameter characterizing the strength of the driving perturbation. Consequently, this is a system of *slow* evolution equations. The phases of the excited g degrees of freedom enter the RHS of this slow system. Therefore, for completeness, we add g equations for the corresponding phase mismatches $\Psi_l \equiv \Theta_l - \Phi_l(t)$ $(l\in I_g)$:

$$\frac{d\Psi_l}{dt} = \frac{d\Theta_l}{dt} - \Omega_l(t) = \omega_l(\lambda) - \Omega_l(t) + O(\varepsilon), \tag{34}$$

where $\omega_l(\lambda)$ is the frequency of the approximating lattice, corresponding to the action variable (see Appendix A) associated with the lth open gap in the main spectrum at time t. These frequencies depend on the local values of the main spectrum components of the approximating lattice and can be evaluated if the evolution of the spectrum is known. We have seen in simulations that synchronization in our system means a continuing satisfaction of resonance condition $\omega_l(\lambda)-\Omega_l(t)\simeq 0$, despite the time variation of the driving frequency $\Omega_l(t)$. We shall see later that the actual frequency difference in the multiphase locked state remains of $O(\varepsilon^{1/2})$. Thus, Eqs. (34) is also a system of *slow* evolution equations.

Our next goal is to analyze our slow system, Eqs. (31) and (34). We observe that $|\psi_n^k|^2$ in Eq. (31) are periodic in variables $\theta_m \equiv 2\pi mn/N - \Theta_m$, i.e., one can Fourier expand

$$|\psi_n^k|^2 = \sum_{\mathbf{m}} b_{\mathbf{m}}^k \exp(i\mathbf{m}\cdot\boldsymbol{\theta}), \tag{35}$$

where coefficients $b_{\mathbf{m}}^k$ depend on λ. We substitute the last expression and the driving force (3) into Eq. (31) and again use the isolated resonances approximation, i.e., leave only the slow (resonant) terms in the resulting equation:

$$\frac{d\lambda_k}{dt} = \frac{1}{\sqrt{N}}\sum_{l\in I_g}\varepsilon_l B_l^k \sin\Psi_l^k. \tag{36}$$

Here B_l^k and σ_l^k are absolute values and complex phases of the corresponding Fourier coefficients, while the phase mismatch $\Psi_l^k = \Theta_l - \Phi_l + \sigma_l^k$ now includes σ_l^k and is viewed as a slow function of time due to the synchronization assumption. We check in Appendix D that the weakly nonlinear limit of Eqs. (31) and (34) yields Eqs. (20) of the weakly nonlinear action-angle formalism. This formalism was used in Sec. III to demonstrate that the multiphase locking in the system is established in the weakly nonlinear limit if the amplitudes of the corresponding driving components exceed the thresholds. Now, we proceed to the analysis of the fully nonlinear stage of synchronized evolution.

In the fully nonlinear stage, all $O(\varepsilon)$ terms (including the new term $d\sigma_l^k/dt$) in Eq. (34) can be neglected compared to $O(\varepsilon^{1/2})$ oscillations of $\omega_k - \Omega_k$ in this equation (see below). Consequently, we omit index l in the phase mismatches in the following. In analyzing the modulational stability of the synchronized evolution, we choose a set of g independent components of the main spectrum, denote these component by Λ_k, and seek solutions of Eqs. (36) and (34) of form $\Lambda_k = \overline{\Lambda_k} + \delta\Lambda_k$ and $\Psi_k = \overline{\Psi}_k + \delta\Psi_k$, where $\overline{\Lambda}_k$ and $\overline{\Psi}_k \ll 1$ are smooth, slow averages, while $\delta\Lambda_k$ and $\delta\Psi_k$ are small and oscillating. We define $\overline{\boldsymbol{\Lambda}}(t)$ by $\omega_k(\overline{\boldsymbol{\Lambda}}) - \boldsymbol{\Omega}_k(t) = \mathbf{0}$ and use them to find $\overline{\Psi}_k$ from the smooth part of Eq. (36):

$$\frac{d\overline{\Lambda}_k}{dt} = \frac{1}{\sqrt{N}}\sum_{l\in I_g}\varepsilon_l \overline{B}_l^k \sin(\overline{\Psi}_l). \tag{37}$$

When the smooth objects are known, the oscillating components are governed by

$$\frac{d(\delta\Lambda_k)}{dt} = -\frac{1}{\sqrt{N}} \sum_{l\in I_g} \varepsilon_l \overline{B_l^k} \delta\Psi_l \tag{38}$$

and

$$\frac{d(\delta\Psi_k)}{dt} = -\sum_{l\in I_g} \frac{\partial\overline{\omega_k}}{\partial\overline{\Lambda_l}} \delta\Lambda_l . \tag{39}$$

By fixing the coefficients in this linear problem locally and seeking solutions of form $\delta\Lambda_k, \delta\Psi_n \sim \exp(-i\nu t)$, we obtain the characteristic equation

$$\mathrm{Det}[M - \nu^2 I] = 0, \tag{40}$$

where

$$M_{km} = \frac{1}{\sqrt{N}} \sum_{l\in I_g} \frac{\partial\overline{\omega_l}}{\partial\overline{\Lambda_m}} \varepsilon_l \overline{B_l^k} \tag{41}$$

and I is the identity matrix. The characteristic equation yields g real frequencies ν_n, all small and of $O(\varepsilon^{1/2})$, if the evolution is stable. Then all $\delta\Lambda_k$ (and, therefore, the amplitudes of oscillatory modulations of the main spectrum components) scale as $O(\varepsilon^{1/2})$, justifying the neglect of $O(\varepsilon)$ terms in Eq. (34). In the *weakly* nonlinear evolution stage, above the thresholds, ν_n are real, while our numerical examples show the continuing phase locking in the system and oscillating modulations of both the main spectrum λ and the frequencies $\omega(\lambda)$ around slowly evolving averages. In order to further test the predictions of our modulational theory, we return to numerics, showing some results in Fig. 7. We excited a two-gap solution in $N=5$ periodic lattice by chirped frequency drives, but stopped the chirping and kept the two driving frequencies constant, $\Omega_{1,2}=2.9$ and 4.36 beyond $t=880$. We used parameters $\alpha_{1,2}=0.0020$, 0.0028 and two sets $\varepsilon_{1,2}=\varepsilon_a=0.135$, 0.08 and $\varepsilon_b=2\varepsilon_a$. Figures 7(a) and 7(c) show the evolution of the main spectrum for the set $\varepsilon_{a,b}$, respectively. As predicted, the averaged evolution of the main spectra is nearly the same for both sets of ε_i. The modulations of λ_i, in contrast, were different. We observed that the open gaps' widths remain constant, in average, beyond $t=880$ and time Fourier analyzed the energy of the resulting quasisteady synchronized state. The power spectra $P(\nu)$ of energy modulations for the two sets of ε_i are shown in Figs. 7(b) and 7(d). We see that, indeed, there exist *two* characteristic frequencies ν_i in the spectrum and both frequencies increase by factor $\sqrt{2}$ when one doubles ε_i. These results illustrate the stability of the synchronized evolution, as well as the predicted $O(\varepsilon^{1/2})$ scaling of the characteristic modulation frequencies.

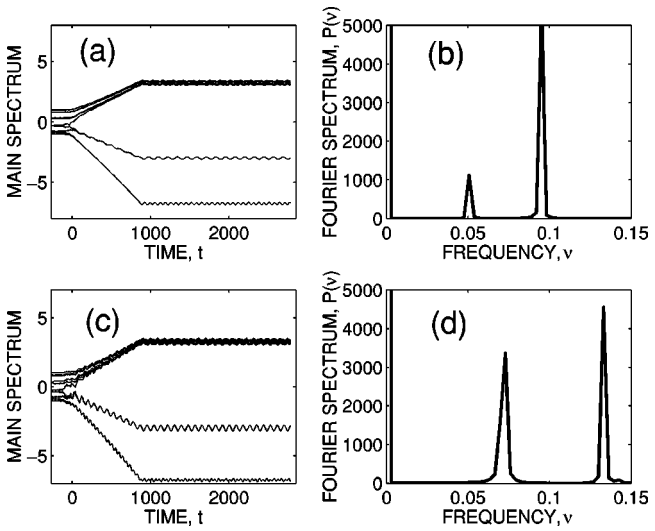

FIG. 7. Modulational stability of synchronized two-gap solution. All driving frequencies remain constant beyond $t=880$. (a), (c): The evolution of the main spectrum for two sets of driving amplitudes: $\varepsilon_{1,2}=\varepsilon_a=0.135$, 0.08 [Fig. 5(a)] and $\varepsilon_{1,2}=\varepsilon_b=2\varepsilon_a$ [Fig. 5(c)]. The power Fourier spectra of energy modulations using drives ε_a (b), and ε_b (d). The characteristic frequencies ν increase by $\sqrt{2}$ when ε_i doubles.

V. CONCLUSIONS

From above, we have made the following conclusions.

(a) We have studied excitation and control of multiphase n-gap solutions of the periodic Toda lattice by synchronization approach. The synchronization was achieved by using a superposition of chirped frequency driving perturbations passing through multiple resonances with the lattice at rest.

(b) The initial, weakly nonlinear stage of evolution of the driven lattice plays an important role in synchronization by passage through resonances. We have shown that in the weakly nonlinear limit the Hamiltonian of the driven Toda lattice is separable in action-angle variables. This enables independent synchronization of each phase of the excited solution with the corresponding driving component, provided the amplitude ε_k of this component exceeds a threshold. All thresholds scale as 3/4 power of the corresponding driving frequency chirp rate.

(c) The synchronization in the system continues beyond the weakly nonlinear stage, as the frequencies of the excited multiphase state of the lattice self-adjust to stay in resonance with all components in the drive, while the solution performs a large excursion in the solutions space in the process of evolution. The time variation of each driving frequency in the synchronized state can be arbitrary (but slow) and independent of other driving frequencies, allowing to cover much of the n-gap solutions space. Thus, we achieve a full control of the excitation by weak forcing and slow variation of external parameters (the driving frequencies).

(d) Our theory predicts that stable synchronized solutions are characterized by $O(\sqrt{\varepsilon})$ oscillating modulations of the main spectrum. The frequencies of these modulations are also small and scale as $O(\sqrt{\varepsilon})$. We have verified this scaling in simulations.

(e) Finally, application of similar synchronization ideas to excitation and control of nontrivial multiphase states in other dynamical and extended systems seems to be an important goal for future research.

ACKNOWLEDGMENTS

This research was supported by the Israel Science Foundation (Grant No. 187/02). One of the authors (M.K.) is grateful to E. Khain for many fruitful discussions.

APPENDIX A: LINEAR LIMIT OF SPECTRAL THEORY

At various stages of the developments in this work we needed objects of the spectral theory in the limit of small amplitude excitations. We find these objects in this appendix.

1. Main spectrum gaps at small excitations

The action-angle variables for the periodic Toda lattice were introduced by Flaschka and McLaughlin [21] and we shall use their results below. We define

$$a_n=\tfrac{1}{2}\exp[-(q_{n+1}-q_n)/2],\ b_n=\tfrac{1}{2}p_n \tag{A1}$$

and write the evolution equations for the unperturbed Toda lattice as

$$\frac{da_n}{dt}=a_n(b_n-b_{n+1}), \tag{A2}$$

$$\frac{db_n}{dt}=2(a_{n-1}^2-a_n^2). \tag{A3}$$

The associated spectral problem uses solutions of these equations as coefficients in the following linear system [12,14]:

$$(L\psi)_n\equiv a_{n-1}\psi_{n-1}+b_n\psi_n+a_n\psi_{n+1}=\lambda\psi_n, \tag{A4}$$

which defines the main spectrum λ, i.e., a combination of two sets of N eigenvalues λ^+ and λ^- corresponding to periodic ($\psi_{n+N}=\psi_n$) and antiperiodic ($\psi_{n+N}=-\psi_n$) boundary, conditions respectively.

Both λ^+ and λ^- are N independent integrals of motion of the periodic lattice. Let us order the main spectrum λ so that $\lambda_1\leqslant\lambda_2\leqslant=\cdots\leqslant\lambda_{2N}$. Then the kth action variable is defined by

$$I_k=(-1)^{N-k}\frac{2}{\pi}\int_{\lambda_{2k}}^{\lambda_{2k+1}}\ln\left|\frac{\Delta(\lambda)+\sqrt{\Delta(\lambda)^2-4}}{2}\right|d\lambda, \tag{A5}$$

where $k=1,2,\ldots,N-1$ and

$$\Delta(\lambda)=2^{2N}\prod_{j=1}^{2N}(\lambda-\lambda_j)+4 \tag{A6}$$

is the discriminant of the spectral problem.

One can easily show that for the lattice at rest ($a_n=1/2$ and $b_n=0$), $\lambda_k^+=\cos(2\pi k/N)$ and $\lambda_k^-=\cos[\pi(2k+1)/N]$ and, therefore, the main spectrum λ is doubly degenerate except for eigenvalues λ_1 and λ_{2N}. Furthermore, in this limit, $\lambda_{2k}=\lambda_{2k+1}=-\cos(\pi k/N)$ for $k=1,2,\ldots,N-1$ and each degenerate pair of the eigenvalues belongs to either λ^+ or λ^- set. The excitation of the lattice may remove the degeneracy and open gaps between the degenerate spectrum components. Let us calculate the width $\delta_k\equiv\lambda_{2k+1}-\lambda_{2k}$ of the kth open gap to lowest order in small amplitude of lattice oscillations.

The orthonormal eigenfunctions of Eq. (A4) for the lattice at rest, corresponding to the degenerate pair of eigenvalues $\lambda_{2k,2k+1}$, $k=1,2,\ldots,N$, are

$$\varphi_{1l}^k=\frac{1}{\sqrt{N}}e^{i\eta_k l},\quad \varphi_{2l}^k=\frac{1}{\sqrt{N}}e^{-i\eta_k l},\quad l=1,\ldots,N, \tag{A7}$$

where $\eta_k=\pi(k+N)/N$. In studying small deviations of the lattice from rest, we introduce small operator $\tilde{L}$

$$(\tilde{L}\cdot\psi)_n\equiv(a_{n-1}-\tfrac{1}{2})\psi_{n-1}+b_n\psi_n+(a_n-\tfrac{1}{2})\psi_{n+1} \tag{A8}$$

or, recalling the definitions (A1),

$$(\tilde{L}\cdot\psi)_n\equiv-\tfrac{1}{4}(q_n-q_{n-1})\psi_{n-1}+\tfrac{1}{2}p_n\psi_n -\tfrac{1}{4}(q_{n+1}-q_n)\psi_{n+1}. \tag{A9}$$

We use $\tilde{L}$ to form matrix

$$\tilde{L}_{ij}^k\equiv\varphi_i^{k\dagger}\cdot\tilde{L}\cdot\varphi_j^k,\quad i,j=1,2. \tag{A10}$$

Then, by the secular perturbation theory, the eigenvalues of $\tilde{L}^k$ are first-order corrections to the degenerate eigenvalues $\lambda_{2k,2k+1}$ of the unperturbed problem.

By using definitions (A7), (A9), (A10), and simple algebra, we find

$$\tilde{L}_{11}^k=\tilde{L}_{22}^k=0,\ \tilde{L}_{21}^k=(\tilde{L}_{12}^k)^* \tag{A11}$$

and

$$\tilde{L}_{12}^k=\frac{1}{2N}\sum_{n=1}^{N}[p_n-2iq_n\sin(\pi k/N)]e^{i2\pi kn/N}. \tag{A12}$$

Since the linear frequencies of the periodic Toda lattice are $\omega_k^0=2\sin(\pi k/N)$ [35],

$$\tilde{L}_{12}^k=(\tilde{L}_{21}^k)^*=\frac{1}{2N}\sum_{n=1}^{N}(p_n-i\omega_k^0q_n)e^{i2\pi kn/N}. \tag{A13}$$

Equations (A11) and (A12) show that the eigenvalues of $\tilde{L}^k$ are equal to $\pm|\tilde{L}_{12}^k|$ and, therefore, the corresponding open gap width is

$$\delta_k\equiv\lambda_{2k+1}-\lambda_{2k}=2|\tilde{L}_{12}^k|. \tag{A14}$$

2. Eigenfunctions

Now, we calculate the eigenfunctions ψ^{2k+1} and ψ^{2k} of system (A9) corresponding to nearly degenerate eigenvalues λ_{2k+1} and λ_{2k}. The secular perturbation theory can be used again, yielding

$$\psi^{2k+1}=\alpha_{11}\varphi_1^k+\alpha_{12}\varphi_2^k \tag{A15}$$

and

$$\psi^{2k}=\alpha_{21}\varphi_1^k+\alpha_{22}\varphi_2^k, \tag{A16}$$

where φ_1^k and φ_2^k are given by Eqs. (A7), and $\alpha_1=(\alpha_{11},\alpha_{12})$ and $\alpha_2=(\alpha_{21},\alpha_{22})$ are normalized eigenvectors of matrix (A10). Then, a straightforward calculation gives

$$\psi^{2k+1}=\frac{1}{\sqrt{2}}(\varphi_1^k-ie^{i\omega_k^0 t}\varphi_2^k) \tag{A17}$$

and

$$\psi^{2k}=\frac{1}{\sqrt{2}}(\varphi_1^k+ie^{i\omega_k^0 t}\varphi_2^k). \tag{A18}$$

3. The action variables

At this stage, we observe that a general solution for the Toda lattice in the linear limit can be written as a superposition of traveling waves:

$$q_n=\sum_{l=1}^{N-1} A_l\cos\left(\frac{2\pi ln}{N}-\omega_l^0 t-\Theta_l^0\right). \tag{A19}$$

Then, it can be shown that each wave component in Eq. (A19) opens exactly *one* gap in the main spectrum. Indeed, by substituting Eq. (A19) into Eq. (A13), we obtain

$$\tilde{L}_{12}^k=\tfrac{1}{2}iA_k\omega_k^0\exp(i\omega_k^0 t) \tag{A20}$$

and, therefore,

$$\delta_k=A_k\omega_k^0. \tag{A21}$$

Next, we relate the linear limit of the kth action variable (A5) to the corresponding open gap width. We expand Eq. (A5) to leading order in δ. We assume (with no loss of generality) that both λ_{2k} and λ_{2k+1} belong to the λ^+ spectrum and use an alternative expression for the discriminant [8]:

$$\Delta(\lambda)\equiv 2^N\prod_{j=1}^{N}(\lambda-\lambda_j^+)+2. \tag{A22}$$

Then, we see that $\lim_{\delta_k\to 0}\Delta(\lambda)=2$ in the region of integration in Eq. (A5). To next order, the integrand in Eq. (A5) can be approximated as

$$\ln\left|\frac{\Delta(\lambda)+\sqrt{\Delta(\lambda)^2-4}}{2}\right|\simeq\sqrt{\Delta(\lambda)-2} \tag{A23}$$

and, therefore,

$$I_k\simeq(-1)^{N-k}\frac{2}{\pi}\int_{\lambda_{2k}}^{\lambda_{2k+1}}\sqrt{\Delta(\lambda)-2}\,d\lambda. \tag{A24}$$

By changing the integration variable in the last integral

$$\lambda=-\frac{\lambda_{2k+1}-\lambda_{2k}}{2}\cos t+\frac{\lambda_{2k+1}+\lambda_{2k}}{2}, \tag{A25}$$

we obtain

$$I_k\simeq\frac{2}{\pi}\int_0^{\pi}\gamma_k\left(\frac{\lambda_{2k+1}-\lambda_{2k}}{2}\right)^2\sin^2 t\,dt, \tag{A26}$$

where

$$\gamma_k=\sqrt{-\frac{2^N\prod_{j=1}^{N}(\lambda-\lambda_j^+)}{(\lambda-\lambda_{2k})(\lambda-\lambda_{2k+1})}}. \tag{A27}$$

To leading order in δ_k, the factor γ_k in integral (A26) is constant,

$$\gamma_k^2=-2^N\prod_{\substack{l=1\\ \lambda_{2k}\neq\lambda_l^+}}^{N}(\lambda_{2k}-\lambda_l^+) \tag{A28}$$

and, therefore,

$$I_k=\tfrac{1}{2}\gamma_k\delta_k^2. \tag{A29}$$

Then, by substituting $\gamma_k=2N/\omega_k^0$ for the unperturbed lattice (see Appendix B), one has

$$I_k=\frac{N}{2\omega_k^0}\delta_k^2. \tag{A30}$$

Finally, by using Eq. (A21), we find $A_k=\sqrt{2I_k/(N\omega_k^0)}$ and, therefore,

$$q_n=\sum_{l=1}^{N-1}\sqrt{\frac{2I_l}{N\omega_l^0}}\cos\left(\frac{2\pi ln}{N}-\omega_l^0 t-\Theta_l^0\right). \tag{A31}$$

APPENDIX B: COEFFICIENTS γ_k

We shall use definitions $\lambda_l^+=\cos(2\pi l/N)$ for the lattice at rest in calculating coefficient γ_k in Eq. (A28). We shall also assume that λ_{2k} in this equation belongs to set λ^+. Then, $\lambda_{2k}=\lambda_m^+=\cos(2\pi m/N)$, where $2m=k+N$, and Eq. (A28) becomes

$$\gamma_k^2=-2^N\prod_{\substack{l=1\\ l\neq m,N-m}}^{N}\left[\cos\left(\frac{2\pi m}{N}\right)-\cos\left(\frac{2\pi l}{N}\right)\right]. \tag{B1}$$

Alternatively, after some algebra,

$$\gamma_k^2=2^{2N-2}\prod_{\substack{l=1\\ l\neq m,N-m}}^{N}\sin^2\left[\frac{\pi(m+l)}{N}\right]. \tag{B2}$$

We use the last expression to write

$$\gamma_k(x)=2^{N-1}\prod_{\substack{l=1\\ l\neq m,N-m}}^{N}\left|\sin\left(\frac{\pi l}{N}+x\right)\right|, \tag{B3}$$

where the definition of $\gamma_k(x)$ is extended to arbitrary $x=\pi m/N+z$. We shall take the limit $z\to 0$ in obtaining the final result. One can rewrite Eq. (B3) as

$$\gamma_k(x)=\frac{2^{N-1}\prod_{l=0}^{N-1}\left|\sin\left(\frac{\pi l}{N}+x\right)\right|}{|\sin z|\left|\sin\left(\frac{2\pi m}{N}+z\right)\right|}. \tag{B4}$$

Finally, we observe that the numerator in Eq. (B4) is equal to (see Ref. [36]) $|\sin(Nx)|=|\sin(Nz)|$ and take the limit $z\to 0$, yielding

$$\gamma_k=\frac{N}{|\sin(2\pi m/N)|}=\frac{2N}{\omega_k^0}. \tag{B5}$$

APPENDIX C: WEAKLY NONLINEAR FREQUENCIES

Here we calculate the diagonal coefficients a_{kk} in the weakly nonlinear frequencies of the Toda lattice,

$$\omega_k=\omega_k^0+\sum_{i=1}^{N-1}a_{ik}I_i. \tag{C1}$$

We use the harmonic decomposition analysis [27] in this calculation. Our starting point is the system of evolution equations for the lattice

$$\frac{d^2q_n}{dt^2}=\exp[-(q_n-q_{n-1})]-\exp[-(q_{n+1}-q_n)]. \tag{C2}$$

We seek a solution of Eq. (C2) in the form of a series of successive approximations, ordered in powers of the amplitude of the leading term in the series:

$$q_n=q_n^{(1)}+q_n^{(2)}+q_n^{(3)}. \tag{C3}$$

We use the ansatz

$$q_n^{(1)}=A_k\cos\Delta_n^k, \tag{C4}$$

where $\Delta_n^k\equiv 2\pi kn/N-\Theta_k$ and $\Theta_k=\omega_k t+\Theta_k^0$, but, unlike the linear case, ω_k includes higher-order corrections, i.e,

$$\omega_k=\omega_k^0+\omega_k^{(1)}+\omega_k^{(2)}. \tag{C5}$$

We shall also set $\omega_k^{(1)}=0$, because, generally, the first correction to the linear frequency is linear in action variables or, equivalently, quadratic in the amplitude of the leading term $q_n^{(1)}$. We substitute our series solution into Eq. (C2) and collect the second-order terms

$$\frac{d^2q_n^{(2)}}{dt^2}=q_{n+1}^{(2)}-2q_n^{(2)}+q_{n-1}^{(2)}-\tfrac{1}{2}[(q_{n+1}^{(1)})^2-(q_{n+1}^{(1)})^2+2q_n^{(1)}q_{n-1}^{(1)}-2q_n^{(1)}q_{n+1}^{(1)}]. \tag{C6}$$

Here, on using Eq. (C4), we obtain

$$\frac{d^2q_n^{(2)}}{dt^2}-q_{n+1}^{(2)}+2q_n^{(2)}-q_{n-1}^{(2)}=\frac{\omega_k^{02}A_k^2}{2}\sin\left(\frac{2\pi k}{N}\right)\sin(2\Delta_n^k), \tag{C7}$$

yielding

$$q_n^{(2)}=\frac{A_k^2}{2\omega_k^{02}}\sin\left(\frac{2\pi k}{N}\right)\sin(2\Delta_n^k). \tag{C8}$$

Next, we collect all third-order terms in Eq. (C2)

$$\frac{d^2q_n^{(3)}}{dt^2}-2\omega_k^0\omega_k^{(2)}q_n^{(1)}=q_{n+1}^{(3)}-2q_n^{(3)}+q_{n-1}^{(3)}-[q_{n+1}^{(1)}q_{n+1}^{(2)}-q_{n-1}^{(1)}q_{n-1}^{(2)}+q_n^{(1)}(q_{n-1}^{(2)}-q_{n+1}^{(2)})+q_n^{(2)}(q_{n-1}^{(1)}-q_{n+1}^{(1)})]-\tfrac{1}{6}[(q_n^{(1)}-q_{n+1}^{(1)})^3+(q_n^{(1)}-q_{n-1}^{(1)})^3], \tag{C9}$$

which, upon using Eqs. (C4) and (C8), gives

$$\frac{d^2q_n^{(3)}}{dt^2}-2\omega_k^0\omega_k^{(2)}q_n^{(1)}-q_{n+1}^{(3)}+2q_n^{(3)}-q_{n-1}^{(3)}=-\frac{A_k^3\omega_k^{02}}{2}\cos\Delta_n^k. \tag{C10}$$

By equating the coefficient in front of the first harmonic terms (with $\cos\Delta_n^k$) in the last equation to zero, one finds

$$\omega_k^{(2)}=\frac{A_k^2\omega_k^0}{4}. \tag{C11}$$

Finally, by relating the amplitude A_k to the corresponding action (see Appendix A), $A_k=\sqrt{2I_k/(N\omega_k^0)}$, we have $\omega_k^{(2)}=I_k/(2N)$, and, therefore,

$$a_{kk}=\frac{1}{2N}. \tag{C12}$$

The analysis above shows that both the cubic and the quartic terms in the expansion of the potential of the lattice in powers of displacements contribute $O(I)$ correction to the frequency. If one keeps only the cubic terms in Eq. (C9), by similar developments, one obtains

$$\frac{d^2q_n^{(3)}}{dt^2}-2\omega_k^0\omega_k^{(2)}q_n^{(1)}-q_{n+1}^{(3)}+2q_n^{(3)}-q_{n-1}^{(3)}$$

$$=-\frac{A_k^3\omega_k^{02}}{2}\cos^2\left(\frac{\pi k}{N}\right)\cos\Delta_n^k \tag{C13}$$

instead of Eq. (C7) and, therefore, an incorrect coefficient

$$a_{kk}=\frac{\cos^2(\pi k/N)}{2N}=\frac{4-\omega_k^{02}}{8N} \tag{C14}$$

in the lowest-order nonlinear frequency of the lattice.

APPENDIX D: WEAKLY NONLINEAR EVOLUTION EQUATIONS

This appendix deals with the weakly nonlinear limit of the slow evolution equations in our spectral theory [see Eqs. (31) and (34)]:

$$\frac{d\lambda_k}{dt}=\tfrac{1}{2}\sum_n f_n|\psi_n^k|^2, \tag{D1}$$

$$\frac{d\Psi_k}{dt}=\omega_k(\lambda)-\Omega_k(t)+O(\varepsilon). \tag{D2}$$

The goal is to reduce these equations to their action-angle counterparts [see Eqs. (20)]:

$$dI_i/dt=\varepsilon_i\sqrt{\frac{I_i}{2\omega_i^0}}\sin\Psi_i, \tag{D3}$$

$$d\Psi_i/dt=\omega_i^0+\frac{I_i}{2N}-\Omega_i(t)+\frac{\varepsilon_i}{2\sqrt{2\omega_i^0 I_i}}\cos\Psi_i. \tag{D4}$$

The equivalence between Eqs. (D2) and (D4) is obvious, thus we discuss the correspondence between Eqs. (D1) and (D3).

A weak excitation of the lattice may remove the degeneracy between eigenvalues λ_{2k} and λ_{2k+1} in the main spectrum and the evolution of $\delta_k\equiv\lambda_{2k+1}-\lambda_{2k}$ is given by

$$\frac{d\delta_k}{dt}=\tfrac{1}{2}\sum_n f_n(|\psi_n^{2k+1}|^2-|\psi_n^{2k}|^2). \tag{D5}$$

Here, the eigenfunctions ψ^{2k+1} and ψ^{2k}, corresponding to λ_{2k+1} and λ_{2k}, are given by Eqs. (A17) and (A18). A simple calculation, based on Eqs. (A17), (A18), and (A7), yields

$$|\psi_n^{2k+1}|^2=\frac{1}{N}\left[1-\sin\left(\frac{2\pi kn}{N}-\omega_k^0 t\right)\right], \tag{D6}$$

$$|\psi_n^{2k}|^2=\frac{1}{N}\left[1+\sin\left(\frac{2\pi kn}{N}-\omega_k^0 t\right)\right]. \tag{D7}$$

Therefore,

$$\frac{d\delta_k}{dt}=-\frac{1}{N}\sum_n f_n\sin\left(\frac{2\pi kn}{N}-\omega_k^0 t\right). \tag{D8}$$

Here, we substitute our forcing [see Eq. (3)]

$$f_n=\frac{1}{\sqrt{N}}\sum_{l\in I_g}\varepsilon_l\cos\left[\frac{2\pi nl}{N}-\Phi_l(t)\right], \tag{D9}$$

where $\Phi_l(t)\approx\omega_l^0 t$ in the phase locked regime. Then, in the isolated resonance approximation,

$$\frac{d\delta_k}{dt}=-\frac{\varepsilon_k}{2\sqrt{N}}\sin\Psi_k. \tag{D10}$$

Finally, by using δ_k from Eq. (A30) in the last equation, we recover Eq. (D3).

[1] A. C. Scott, *Nonlinear Science: Emergence and Dynamics of Coherent Structures* (Oxford University Press, Oxford, 1999).
[2] S. Novikov, S. V. Manakov, L. P. Pitaevskii, and V. E. Zakharov, *Theory of Solitons* (Consultants Bureau, New York, 1983).
[3] L. Friedland, Phys. Rev. E **55**, 1929 (1997).
[4] L. Friedland, Phys. Plasmas **5**, 645 (1998).
[5] L. Friedland and A.G. Shagalov, Phys. Rev. Lett. **81**, 4357 (1998).
[6] L. Friedland and A.G. Shagalov, Phys. Rev. Lett. **85**, 2941 (2000).
[7] L. Friedland and A.G. Shagalov, Phys. Rev. Lett. **90**, 074101 (2003).
[8] M. Toda, *Theory of Nonlinear Lattices* (Springer, New York, 1981).
[9] N.J. Zabusky and M.D. Kruskal, Phys. Rev. Lett. **15**, 240 (1965).
[10] J. Ford, Phys. Rep. **213**, 271 (1992).
[11] M. Henon, Phys. Rev. B **9**, 1921 (1974).
[12] H. Flaschka, Phys. Rev. B **9**, 1924 (1974).
[13] H. Flaschka, Prog. Theor. Phys. **51**, 703 (1974).
[14] S.V. Manakov, Zh. Eksp. Teor. Fiz. **67**, 543 (1974) [Sov. Phys. JETP **40**, 269 (1975)].
[15] A.M. Bloch, Physica D **141**, 297 (2000).
[16] K. Ullmann, A.J. Lichtenberg, and G. Corso, Phys. Rev. E **61**, 2471 (2000); T. Prosen and D.K. Campbell, Phys. Rev. Lett. **84**, 2857 (2000).
[17] K.Ø. Rasmussen, Boris A. Malomed, A.R. Bishop, and Niels Grønbech-Jensen, Phys. Rev. E **58**, 6695 (1998).
[18] Y. Kubota and T. Odagaki, Phys. Rev. E **61**, 3133 (2000).
[19] N. Theodorakopoulos, M. Peyrard, Phys. Rev. Lett. **83**, 2293 (1999).
[20] E. Date and S. Tanaka, Prog. Theor. Phys. **59**, 457 (1976);

Prog. Theor. Phys. Suppl. **59**, 107 (1976).
[21] H. Flaschka and D.W. McLaughlin, Prog. Theor. Phys. **55**, 438 (1976).
[22] L. Friedland, Phys. Rev. E **59**, 4106 (1999).
[23] J. Fajans, E. Gilson, and L. Friedland, Phys. Rev. Lett. **82**, 4444 (1999).
[24] L. Friedland, Phys. Rev. E **61**, 3732 (2000).
[25] L. Friedland, Astrophys. J. Lett. **547**, L75 (2001).
[26] E. Grosfeld and L. Friedland, Phys. Rev. E **65**, 046230 (2002).
[27] L. D. Landau and E. M. Lifshitz, *Course of Theoretical Physics: Vol. 1 Mechanics* (Pergamon, Oxford, 1959).
[28] MATHEMATICA, Version 4.0, Wolfram Research Inc., Champaign, IL, 1999.
[29] J. Ford, J. Math. Phys. **2**, 387 (1961).
[30] J. Ford and J. Waters, J. Math. Phys. **4**, 1293 (1963).
[31] E.A. Jackson, J. Math. Phys. **4**, 551 (1963); **4**, 686 (1963).
[32] M. Henon and C. Heiles, Astron. J. **69**, 73 (1964).
[33] R. Z. Sagdeev, D. A. Usikov, and G. M. Zaslavsky, *Nonlinear Physics: From Pendulum to Turbulence and Chaos* (Harwood Academic Publishers, New York, 1988), p. 116.
[34] I.M. Krichever, Sov. Math. Dokl. **270**, 1312 (1983).
[35] W.E. Ferguson, Jr., H. Flaschka, and D.W. McLaughlin, J. Comput. Phys. **45**, 157 (1982).
[36] I. S. Gradsteyn and I. M. Ryzhik, *Table of Integrals, Series, and Products* (Academic Press, New York, 1980), p. 33.